

Genetic variation in *YIGE1* contributes to ear length and grain yield in maize

Yun Luo^{1*} , Mingliang Zhang^{1*} , Yu Liu¹, Jie Liu^{1,2} , Wenqiang Li¹, Gengshen Chen¹, Yong Peng¹ , Min Jin¹, Wenjie Wei¹ , Liumei Jian¹ , Jin Yan¹, Alisdair R. Fernie³  and Jianbing Yan^{1,4} 

¹National Key Laboratory of Crop Genetic Improvement, Huazhong Agricultural University, Wuhan 430070, China; ²Wisconsin Institutes for Discovery, University of Wisconsin-Madison, Madison, WI 53715, USA; ³Department of Molecular Physiology, Max-Planck-Institute of Molecular Plant Physiology, Am Mühlenberg 1, Potsdam-Golm 14476, Germany; ⁴Hubei Hongshan Laboratory, Wuhan 430070, China

Summary

Author for correspondence:
Jianbing Yan
Email: yjianbing@mail.hzau.edu.cn

Received: 1 November 2021
Accepted: 18 November 2021

New Phytologist (2022) 234: 513–526
doi: 10.1111/nph.17882

Key words: auxin, ear length, grain yield, inflorescence meristem, maize, sugar, *YIGE1*.

- Ear length (EL), which is controlled by quantitative trait loci (QTLs), is an important component of grain yield and as such is a key target trait in maize breeding. However, very few EL QTLs have been cloned, and their molecular mechanisms are largely unknown.
- Here, using a genome wide association study (GWAS), we identified a QTL, *YIGE1*, which encodes an unknown protein that regulates EL by affecting pistillate floret number. Over-expression of *YIGE1* increased female inflorescence meristem (IM) size, increased EL and kernel number per row (KNPR), and thus enhanced grain yield. By contrast, CRISPR/Cas9 knockout and *Mutator* insertion mutant lines of *YIGE1* displayed decreased IM size and EL.
- A single-nucleotide polymorphism (SNP) located in the regulatory region of *YIGE1* had a large effect on its promoter strength, which positively affected EL by increasing gene expression. Further analysis shows that *YIGE1* may be involved in sugar and auxin signal pathways to regulate maize ear development, thus affecting IM activity and floret production in maize inflorescence morphogenesis.
- These findings provide new insights into ear development and will ultimately facilitate maize molecular breeding.

Introduction

Maize provides 42% of the world-wide food calories consumed by humans, and in doing so it has exceeded the consumption of rice to become the world's most important cereal crop (Hawkins *et al.*, 2013). By 2050, a 50% increase in cereal grain production will be required to meet the needs of the estimated human population of *c.* 9.7 billion (Ray *et al.*, 2013; Gerland *et al.*, 2014; Yu & Li, 2021). Thus, higher yield remains a major goal in maize crop breeding. Ear length (EL) is an important component of yield, with an increased EL leading to a higher grain yield (Huo *et al.*, 2016; Jia *et al.*, 2020). However, identification of the genetic components underlying EL has proven challenging. To date, hundreds of quantitative trait loci (QTLs) for EL have been identified (Xiao *et al.*, 2016; Li *et al.*, 2018), but few have been cloned (Jia *et al.*, 2020; Ning *et al.*, 2021).

Traditional QTL identification in plants depends on synthetic population-based linkage analysis or natural population-based linkage disequilibrium (LD) analysis. Linkage analysis is resource- and time-consuming, given that large population size, high-resolution linkage maps and reliable phenotypes are required to ensure the accuracy of detection. Moreover, in a QTL mapping population, the limited number of recombination events leads to

large confidence intervals comprising many genes, which render it difficult to identify the causal gene(s) underlying a QTL (Price, 2006; Liang *et al.*, 2021). Conversely, genome wide association studies (GWAS) can resolve QTLs to the genic level by taking advantage of historical recombination. Its widespread adoption has led to a rapid explosion in the identification of trait-associated variations or putative candidate genes for complex traits, especially in maize, which is characterized by rapid LD decay (Flint-Garcia *et al.*, 2003; Yan *et al.*, 2011). Indeed, the use of GWAS has facilitated the genetic dissection of many different traits in maize, from simple, relatively quantitative traits, including flowering time (Hung *et al.*, 2012; Yang *et al.*, 2013) and nutritional content (Yan *et al.*, 2010; Li *et al.*, 2013), to complex quantitative traits, including drought tolerance (Mao *et al.*, 2015; Wang *et al.*, 2016), kernel size and weight (Liu *et al.*, 2017) and grain moisture (Li *et al.*, 2021). However, GWAS have a lower power of detection for low-frequency variants and QTLs with minor effects and often generates false positives due to inherent population structure (Flint-Garcia *et al.*, 2005; Zhang *et al.*, 2010; Xiao *et al.*, 2016). Surprisingly, although association studies of maize EL have been attempted (Xiao *et al.*, 2016; Zhu *et al.*, 2018), few causal genes have been identified.

Auxin regulates inflorescence development by affecting initiation and formation of axillary meristems (Zhao, 2010; Zhang & Yuan, 2014). A *PINOID*-related kinase gene, *BIF2*

*These authors contributed equally to this work.

(McSteen & Hake, 2001; McSteen *et al.*, 2007), and two *AUXIN/INDOLE-3-ACETIC ACID* (*AUX/IAA*)-related genes, *BIF4* and *BIF1* (Galli *et al.*, 2015), regulate inflorescence axillary meristem initiation and determinacy. A PIN-FORMED-related gene, *ZmPIN1*, functions as an auxin efflux transporter (Gallavotti *et al.*, 2008b), which was shown to be directly regulated by *BIF2* to affect maize branching during maize inflorescence development (Skirpan *et al.*, 2009). Two auxin biosynthesis genes, *SPI1* (Gallavotti *et al.*, 2008a) and *VT2* (Phillips *et al.*, 2011), are required for inflorescence development. Moreover, *KRN6* positively regulates EL and functions in auxin-dependent inflorescence development by mediating Arf GTPase-activating protein (AGAP) phosphorylation (Jia *et al.*, 2020). Thus, auxin plays a critical role in the regulation of axillary meristem initiation and EL in maize. Similarly, it has been demonstrated that sugar could act as a signal in a specific pathway to regulate plant growth. The maize *ra3* gene, which operates upstream of *ra1*, appears to regulate inflorescence development by modulating sugar signaling (Satoh-Nagasawa *et al.*, 2006). Although the fact that this mutation can be complemented by an inactive version of *ra3* suggests that the mechanism underlying this phenotypic change may be unrelated to the enzymatic activity, Claeys *et al.* (2019) suggest that we do not fully understand the mechanisms underlying this phenomenon. That said, recent evidence suggests that sugar could affect kernel (LeClere *et al.*, 2010), root (Yuan *et al.*, 2020), and bud (Bertheloot *et al.*, 2020) growth via the regulation of auxin signaling in plants. However, as yet, little is known about the interaction between sugar signaling and auxin signaling in maize inflorescence morphogenesis.

In this study we mapped *qEL1*, a major QTL for EL on chromosome 1, using a GWAS and cloned the underlying functional gene (*GRMZM2G008490* in B73 Ref_V2), which we named *YIGE1*. It is found that *YIGE1* positively affects EL via the elevation of auxin concentrations, IM activity and floret production. The inbred lines which contain the favorable allele of *qEL1* showed greater promoter activity, higher expression of *YIGE1*, and elevated EL. Our analyses revealed that *YIGE1* underwent continuous selection during maize selection, and that the favorable haplotype is considerably enriched in modern maize. These findings thus provide beneficial information for future maize improvement.

Materials and Methods

Candidate gene identification by genome wide association study analysis

A total of 540 diverse inbred lines from the association mapping panel were genotyped with 1.25 million single-nucleotide polymorphism (SNP) markers (Yang *et al.*, 2011; Liu *et al.*, 2017b). Ear length for this population was evaluated in five environments, which have been described previously (Yang *et al.*, 2014). The GWAS was performed using TASSEL v.3.0 (Bradbury *et al.*, 2007) with a mixed linear model (MLM) considering varietal relatedness (K) and population structure (Q) (MLM+K+Q) (Yu *et al.*, 2006; Zhang *et al.*, 2010). The LD among

associated SNPs was calculated using HAPLOVIEW v.4.1 (Barrett *et al.*, 2005).

Transgenic verification

To knock out four candidate genes, we designed two guide RNAs targeting the exon for each gene with CRISPR-P (Liu *et al.*, 2017a) (<http://crispr.hzau.edu.cn/CRISPR2/>) and cloned them into pCPBZmUbi-hspCas9 (Li *et al.*, 2017). For overexpression of *YIGE1*, the full-length coding sequence (CDS) of *YIGE1* infused with yellow fluorescent protein (YFP) was driven by the ubiquitin promoter. Both the overexpression and CRISPR-Cas9 vectors were transformed into KN5585 (Liu *et al.*, 2020) with *Agrobacterium tumefaciens* EHA105 (Weimi Biotechnology Co. Ltd, Changzhou, China), and the positive lines and editing events were confirmed through polymerase chain reaction (PCR) analysis. The primers used are listed in Supporting Information Table S1. The transgenic lines were planted in experimental fields in Hainan (Sanya; 18.3°N, 109.5°E) and Hubei (Wuhan; 30.58°N, 114.31°E), China. Plants were grown in 2.5 m rows, spaced 0.5 m apart, with 11 individuals in each row.

YIGE1 mutant screening

The maize *mum1* mutant of *YIGE1* (mu1032507), a *Mutator*-mediated mutant, was obtained from the Maize Stock Center (<https://maizecoop.cropsci.uiuc.edu/>). The *Mu* insertion was confirmed by PCR with *YIGE1*-specific and TIR6 primers (Table S1). Heterozygous individuals were backcrossed to wild-type (WT) individuals twice and segregated through self-pollination. Approximately 80 individuals were evaluated for both the homozygous *mum* mutants and the WT siblings in experimental fields in Hebei (Baoding; 39.1°N, 115.3°E) and Hubei (Ezhou; 30.1°N, 114.4°E).

Phenotype measurement

We collected maize ears before and after pollination from WT, *mum1* mutant, *YIGE1* overexpression (OE) and nontransgenic (NT) lines, counted the number of florets per row, and measured ear length with ruler. We obtained a picture of the inflorescence meristem (IM) on each developing ear (3–4 mm) using a stereomicroscope (Olympus; SZX10) and measured the size of the IM using IMAGEJ (Schindelin *et al.*, 2015).

Luciferase activity assay

To test the effect of variations in the *YIGE1* promoter on gene expression, a dual-luciferase transient expression assay was performed in maize protoplasts (Huang *et al.*, 2018). In this system, the reporter construct contains two luciferase cassettes, one being the Renilla luciferase (REN) reporter gene driven by the 35S promoter, which is used as an internal control, and the other being firefly luciferase (LUC) driven by the target gene promoter. Promoter sequences of *YIGE1* (c. 1.5 kb in length) were amplified from maize inbred lines YU87-1 and BK. The primers for amplifying the

YIGE1 promoter sequences are listed in Table S1. Point mutation promoter sequences were synthesized by Tsingke Biological Technology Co. Ltd (Wuhan, China). These four promoter sequences were then cloned into the pGreen II 0800-LUC vector, upstream of mpCaMV, to generate the reporter constructs. Mesophyll protoplasts were isolated from the leaves of 10-d-old etiolated B73 seedlings. Subsequently, the prepared plasmids were transformed into the prepared mesophyll protoplasts using polyethylene glycol-mediated transformation (Yoo *et al.*, 2007). Both firefly LUC and REN activity was measured using the Dual-Luciferase Reporter Assay System (Promega) according to the manufacturer's instructions. The LUC activity of each construct was measured with three technical replicates for each of three biological replicates. Relative LUC activity was calculated by normalizing the firefly LUC activity to the Renilla LUC activity.

In situ hybridization

Developing ears (2–5 mm) from B73 were fixed in formalin–acetic acid–alcohol (FAA) solution for 16 h at 4°C, which was then replaced with 70% ethanol twice and dehydrated with an ethanol series, substituted with xylene, embedded in Paraplast Plus (Sigma), and sectioned to a thickness of 8 µm. Two probes of 860 and 895 bp RNA fragments were synthesized using SP6 and T7 RNA polymerase (Roche), respectively, with digoxigenin-UTP as a label. RNA hybridization and immunological detection of the hybridized probes were performed as described previously (Lincoln *et al.*, 1994; Jackson & Hake, 1999), with the addition of 8% polyvinyl alcohol to the detection buffer to minimize diffusion of the reaction products. Slides were exposed for 12–15 h before mounting and imaging, followed by visualization under a microscope (Eclipse 80i; Nikon, Tokyo, Japan). The primers used for the RNA probes are listed in Table S1.

Quantitative real-time polymerase chain reaction (qRT-PCR) and RNA-seq

For qRT-PCR analysis, c. 0.1 g of plant tissue was used to extract total RNA using Quick RNA Isolation Kit (Huayueyang Biotechnology Co. Ltd, Beijing, China). Sources of the analyzed tissue included immature ears (2–5 mm) from *YIGE1*-OE, *mum1* and 82 inbred lines, and stem, bract, immature roots, leaves, immature leaves, developing tassels, and developing ears (2, 2–5 and 5–8 mm) from WT and *mum1*. EasyScript One-Step gDNA Removal and cDNA Synthesis SuperMix (TransGen Biotech Co. Ltd, Beijing, China) was used to remove the gDNA from the extracted RNA and synthesize first-strand complementary DNA. Real-time fluorescence quantitative polymerase chain reaction with SYBR Green Master Mix (Vazyme Biotech Co. Ltd, Nanjing, China) on a CFX96 Real-Time System (Hercules, CA, USA) was used to quantify the expression level of *YIGE1*. Each set of experiments was repeated three times, and the relative quantification method ($2^{-\Delta\Delta CT}$) (Rao *et al.*, 2013) was used to evaluate relative expression, with maize *ACTIN* (*Zm00001d010159*) used as the internal control. The primers used for quantitative PCR are listed in Table S1.

For RNA-seq analysis, the RNA extracted from developing ears (0.5–1 mm) of *YIGE1*-OE and nontransgenic lines, with three biological replicates for each genotype, were used for RNA-Seq (Annoroad Gene Technology, Beijing, China). Total RNA was isolated using the Quick RNA Isolation Kit (Huayueyang Biotechnology Co. Ltd). A library with insert sizes ranging from 200 to 500 bp was prepared using commercial library preparation kits (TruSeq Stranded mRNA LT-SetA, RS-122-1201; Illumina, San Diego, CA, USA) and was sequenced following the HiSeq X-Ten protocols. Low sequencing quality reads and adapter sequences were removed using the software TRIMMOMATIC v.0.36 (Bolger *et al.*, 2014). The paired-end reads were mapped onto the B73 AGPv.3.25 reference genome using the software TOPHAT2 (Kim *et al.*, 2013); only the uniquely mapped reads were used to quantify gene expression levels using CUFFLINKS (Ghosh & Chan, 2016). The expression data for each gene was normalized using the software DESEQ2 (Varet *et al.*, 2016) before the subsequent analysis. Differential gene expression was determined using EDGER. Enrichment analysis of gene ontology (GO) was performed using the AGRI GO v.2.0 software (Tian *et al.*, 2017) (<http://systemsbiology.cau.edu.cn/agriGOv2/>). Gene ontology terms with $P < 0.01$ were identified as enriched processes. The expression of selected genes that are critical in maize development was quantified by qRT-PCR to verify the RNA-seq data.

Detection of sugar and phytohormones

Fresh developing ears (2–5 mm) from *YIGE1* OE and NT lines were harvested, immediately frozen in liquid nitrogen and stored at –80°C. Sugar and phytohormone content was detected using METWARE (<http://www.metware.cn/>).

For the detection of sugar, the freeze-dried developing ears were crushed using a mixer mill (MM 400; Retsch, Haan, Germany) with a zirconia bead for 1.5 min at 30 Hz. Twenty milligrams of powder was dissolved in 500 µl of methanol: isopropanol: water (3 : 3 : 2, v/v/v), vortexed for 3 min and ultrasonicated for 30 min. The extract was centrifuged at 18 400 g at 4°C for 3 min. Next, 50 µl of the supernatant was mixed with 20 µl internal standard (ribitol, 100 µg ml⁻¹) and evaporated under a nitrogen gas stream. The evaporated sample was transferred to the lyophilizer for freeze-drying, and the residue was used for further derivatization. The residue was mixed with 100 µl solution of methoxyamine hydrochloride in pyridine (15 mg ml⁻¹), and the mixture was incubated at 37°C for 2 h. Next, 100 µl of *N,O*-Bistrifluoroacetamide (BSTFA) was added into the mixture and kept at 37°C for 30 min after vortex-mixing. The mixture was analyzed by gas chromatography mass spectrometry (GC-MS) after diluting to an appropriate concentration. A 7890B gas chromatograph (Agilent, Palo Alto, CA, USA) coupled to a 7000D mass spectrometer (Agilent) with a DB-5MS column (30 m length × 0.25 mm internal diameter × 0.25 µm film thickness; J&W Scientific, Milwaukee, WI, USA) was used for the GC-MS analysis (Gómez-González *et al.*, 2010; Dauphin *et al.*, 2020).

For the detection of phytohormones, 50 mg of plant sample material was weighed, placed into a 2 ml plastic microtube,

frozen in liquid nitrogen, and dissolved in 1 ml methanol : water : formic acid (15 : 4 : 1, v/v/v). For quantification, 10 µl internal standard mixed solution (100 ng ml⁻¹) was added to the extract. The mixture was vortexed for 10 min, followed by centrifugation for 5 min (18400 g at 4°C). The supernatant was then transferred to a clean plastic microtube, evaporated to dryness, re-dissolved in 100 µl 80% methanol (v/v), and filtered through a 0.22 µm membrane filter for further liquid chromatography–tandem mass spectrometry (LC-MS/MS) analysis. An ultra-performance liquid chromatography-electrospray ionization tandem mass spectrometry (UPLC-ESI-MS/MS) system (the UPLC system was an ExionL™ AD; Sciex (Washington, DC, USA); the MS system was a 6500 Triple Quadrupole; Applied Biosystems; Redwood, CA, USA) was employed for LC-MS/MS analysis (Floková *et al.*, 2014; Li *et al.*, 2016; Shimura *et al.*, 2018).

Results

YIGE1 positively regulates maize ear length

In a widely used maize association mapping panel (Yang *et al.*, 2011, 2014; Xiao *et al.*, 2017), we found that EL shows large variations, ranging from 7.25 to 17.41 cm, with an average of 12.24 cm (Fig. S1). Using a new and high density SNP marker set (1.25 million SNPs, minor allele frequency (MAF) ≥ 0.05; Liu *et al.*, 2017b), a QTL (*qEL1*) on chromosome 1 was found to be significantly associated with EL ($P < 9.87 \times 10^{-7}$) by performing a GWAS, controlling for both the population structure and kinship (MLM, Q + K; Yu *et al.*, 2006; Zhang *et al.*, 2010; Fig. 1a). Moreover, a QTL was also identified in the equivalent region in a recombinant inbred line (RIL) population derived from cross between YU87-1 (with shorter EL) and BK (with longer EL; Xiao *et al.*, 2016). Four annotated genes were identified in the candidate region (Fig. 1a). We measured the expression levels of these four genes in 2–5 mm developing ears in the two parental lines of the RIL population. Of the four genes, two showed no difference in expression levels, while genes *GRMZM2G329040* and *GRMZM2G008490* showed nearly two-fold higher expression in BK than in YU87-1 (Fig. 1a).

In order to confirm the identity of the gene governing EL variation, we used CRISPR/Cas9 technology to knock out these four genes. Notably, only *GRMZM2G008490* knockout (KO) lines carrying a 432 bp deletion in their CDS, which results in a deletion of 144 amino acids (Fig. S2a,b), displayed significantly decreased EL (1.09 cm shorter compared with the negative control; $P = 3.83 \times 10^{-5}$, $n = 59/69$; Figs 1b,c; S2c). Knockout lines of the other three genes were invariant in EL compared with their respective controls (Fig. S3). In addition, we used *mum1* lines, which have a *Mutator* insertion at 1347 bp upstream of ATG and OE lines of *GRMZM2G008490* driven by the ubiquitin promoter to further validate the function of *GRMZM2G008490*. Compared with wild-type (WT) plants, *mum1* mutants displayed both significantly reduced expression levels (Fig. 1d) and shorter EL (Figs 1e,f; S4). By contrast, the OE lines had significantly increased expression levels (Figs 1g; S5a) and longer EL (Figs 1h, i; S5b) than that of nontransgenic (NT) siblings in four

independent transgenic events. Taken together, these data indicate that *GRMZM2G008490* (*Zm00001d028915* in B73 Ref_V4), which we refer to as *YIGE1* hereafter, is the causal gene for *qEL1* and positively regulates EL.

YIGE1 encodes an unknown protein with only one predicted exon. Rapid amplification of cDNA ends (RACE)-polymerase chain reaction (PCR) indicated that the full-length *YIGE1* cDNA consisted of a 183-bp 5' UTR, a 1704-bp open reading frame (ORF; one exon) and a 159-bp 3' UTR (Fig. S6a,b). We searched for proteins homologous to *YIGE1* in the National Center for Biotechnology Information database, and found that the closest orthologs of *YIGE1*, in *Sorghum bicolor*, have not been functionally characterized (Fig. S6b). However, a close homolog, which is named HCF243 and shares 38.5% amino acid identity with *YIGE1*, was identified in Arabidopsis. HCF243 has been reported to encode a chloroplast-localized protein and to be involved in D1 protein stability of the photosystem II complex, with its mutant displaying high Chl fluorescence, resulting in shorter inflorescence stems and pale rosette leaves (Zhang *et al.*, 2011). However, *YIGE1* has a different subcellular localization (in the cytoplasm; Fig. S6c). In addition, KO, OE, and *mum1* lines of *YIGE1* had normal growth without pale leaves (Fig. S7). Therefore, *YIGE1* may have different functions in different plants (e.g. maize vs Arabidopsis).

A single SNP in the putative *YIGE1* promoter region contributes to the expression and ear length variation

To determine the functional polymorphism, we re-sequenced a 4 kb region covering the regulatory region and gene body of *YIGE1* in 448 diverse inbred lines which belong to the association mapping population (Yang *et al.*, 2011). In total, 102 SNPs and 27 insertions/deletions (InDels) were identified. Candidate gene association analysis with these markers revealed that four SNPs in the promoter, eleven SNPs – including nine nonsynonymous and two synonymous variations – in the exon, and two SNPs in the 3'-UTR (Fig. S8) were significantly associated with EL, among which the lead SNP Chr1.S_50679974 had the lowest *P*-value ($P = 4.3 \times 10^{-4}$; Fig. 2a). All of the significant polymorphisms are located within one LD block ($r^2 > 0.50$; Fig. 2a). Conditional association analysis, which used Chr1.S_50679974 as a covariant, found no other significant SNPs (Fig. S9). This implied that only one causal variant existed within this gene. In addition, *YIGE1* expression levels in 2–5 mm immature ears of 82 inbred lines were positively correlated with EL (Pearson's $r = 0.53$, $P = 1.12 \times 10^{-6}$; Figs 2b; S10). Considering that *YIGE1* expression was significantly associated with EL, and the most significant SNP, Chr1.S_50679974, was located in a promoter region, we speculated that causal variation should come from this regulatory region. Moreover, lines harboring C at Chr1.S_50679974 showed higher expression levels of *YIGE1* and longer EL (Fig. 2c,d) than that of lines harboring T. These observations agree with the phenotypic changes observed in the OE and *mum1* lines, suggesting that Chr1.S_50679974 was the most likely functional polymorphism for variation of *YIGE1* expression and EL across a wide range of maize germplasm.

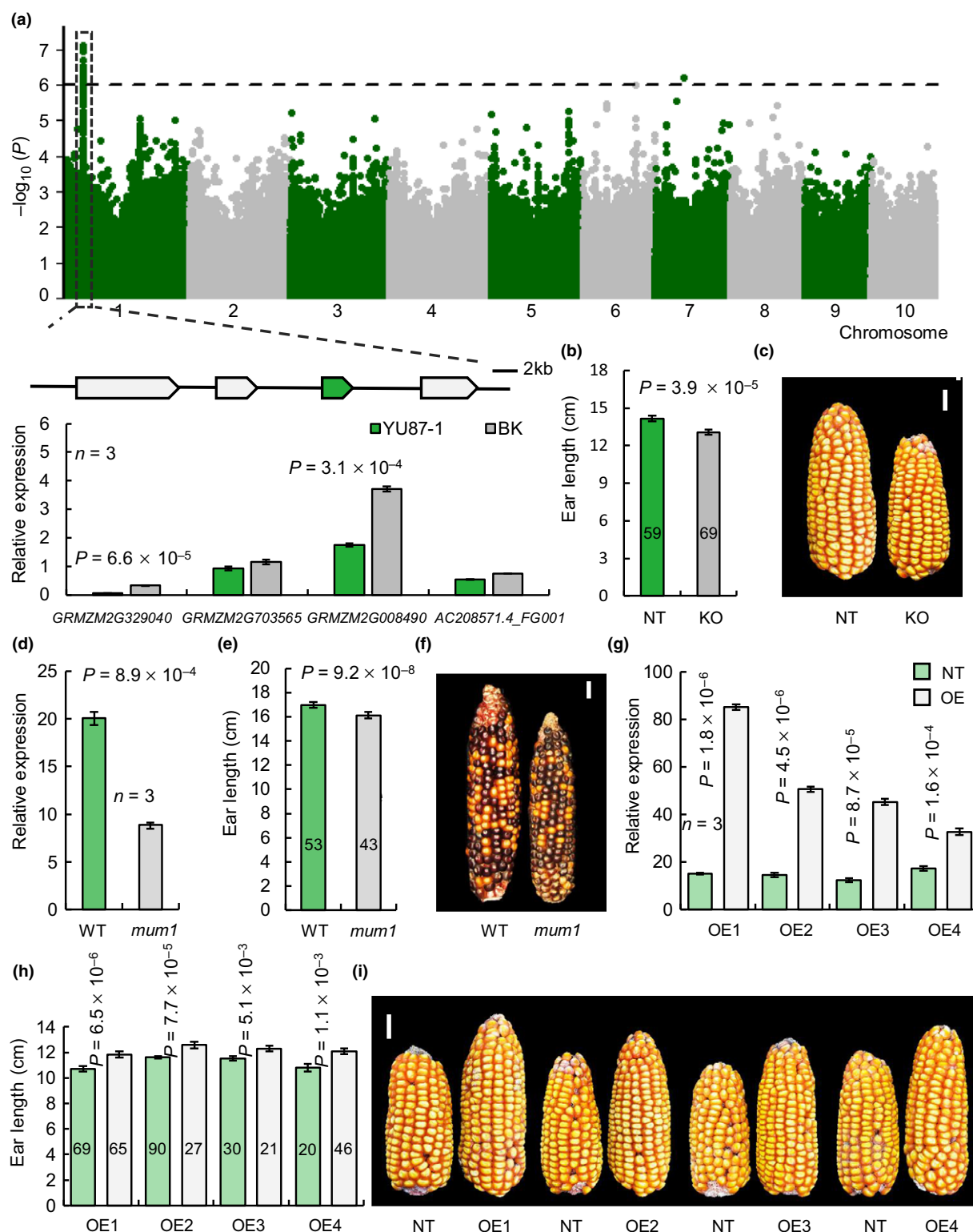


Fig. 1 Identification and validation of a major ear length (EL) quantitative trait locus (QTL) in maize. (a) Manhattan plot for a genome wide association study (GWAS) on EL from the maize association mapping panel. The black horizontal dashed line indicates the threshold for the GWAS ($P < 9.87 \times 10^{-7}$). The locations of the predicted open reading frames (ORFs) in B73 Ref_V2 are indicated. The expression levels of four candidate genes in 2–5 mm developing ears in the YU87-1 and BK lines were measured using quantitative real-time polymerase chain reaction (qRT-PCR), with three biological replicates for each gene. (b, c) Ear length of knockout lines. (d, e) *GRMZM2G008490* relative expression (d) and EL (e, f) for wild-type (WT) and *mum1* mutant plants. (g–i) *GRMZM2G008490* relative expression (g) and EL (h, i) for nontransgenic (NT) and overexpression (OE) lines. The data in (a, b, d, e, g, h) are means \pm SE. The numbers in each column indicate the sample sizes. The level of significance was determined using one-way analysis of variance (ANOVA). Bars: (c, f, i) 3 cm.

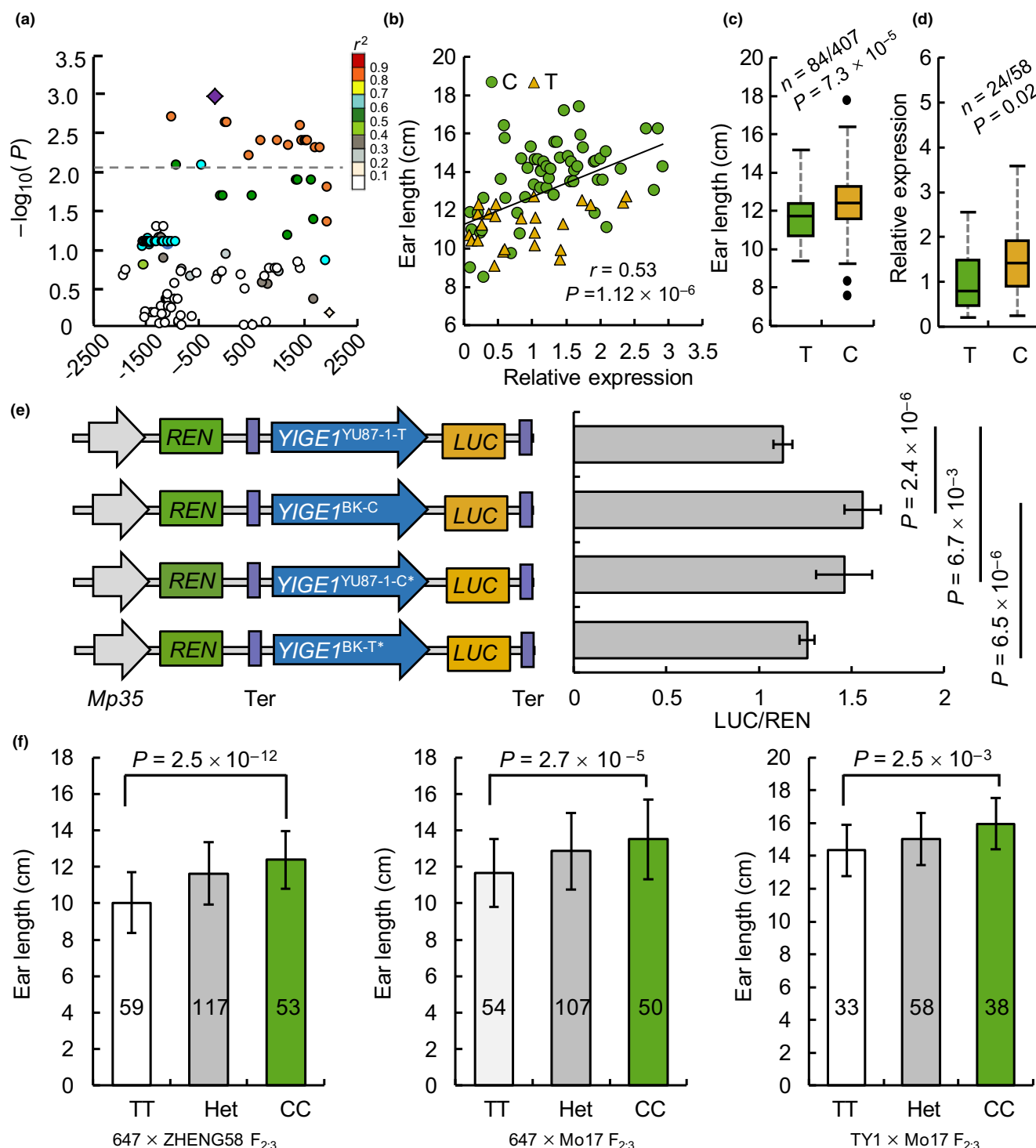


Fig. 2 One single-nucleotide polymorphism (SNP) affects ear length (EL) and *YIGE1* expression. (a) The association analysis of genetic variation in *YIGE1* and EL. The lead SNP is shown with a purple diamond, and the other SNPs are colored according to their linkage disequilibrium (LD; r^2 value) with the lead SNP. The horizontal dash-dot line indicates the threshold. The vertical axis indicates $-\log_{10}$ transformed observed P -values. (b) The correlation between expression of *YIGE1* and EL. (c) Box-and-whisker plots of EL of 84 lines harboring homozygous T and 407 inbred lines containing homozygous C at Chr1.S_50679974. (d) Expression levels of *YIGE1* in 24 inbred lines harboring homozygous T and 58 inbred lines containing homozygous C. Each box in (c, d) represents the median and interquartile range, and whiskers extend to maximum and minimum values. (e) Schematic diagrams of the *YIGE1* construct are shown on the left. On the right, the boxplot shows the activity of four different promoters. *YIGE1*^{BK} represents the promoter of BK with allele C at Chr1.S_50679974, and *YIGE1*^{YU87-1} represents the promoter of YU87-1 with allele T at Chr1.S_50679974. *YIGE1*^{YU87-1-C*}, and *YIGE1*^{BK-T*} represent the point mutation at Chr1.S_50679974 for *YIGE1*^{YU87-1} and *YIGE1*^{BK}, respectively. LUC, firefly luciferase; REN, Renilla luciferase. (f) The lead SNP Chr1.S_50679974 co-segregated with EL in three F_{2:3} populations. The numbers in each column indicate the sample sizes. The data in (e, f) are mean values \pm SE, and P -values were calculated using one-way analysis of variance (ANOVA).

To explore the effect of Chr1.S_50679974 on expression of *YIGE1* and EL, we next measured the activity of LUC driven by promoters harboring different alleles of Chr1.S_50679974 in the maize protoplast. As expected, LUC driven by the *YIGE1* promoter from *YIGE1*^{BK} (C allele) had much higher LUC activity than that from *YIGE1*^{YU87-1} (T allele; Fig. 2e), indicating that the C allele contributed to the higher expression of *YIGE1*^{BK}. Next, point mutation of the *YIGE1* promoter by substitution of the T allele of *YIGE1*^{YU87-1} with the C allele significantly elevated the promoter activity (Fig. 2e). Conversely, substitution of the C allele of *YIGE1*^{BK} with the T allele resulted in reduced promoter activity (Fig. 2e). Moreover, three F₂:₃ segregation populations were generated by the crossing of longer (ZHENG58 and Mo17, C allele) and shorter (647 and TY1, T allele) EL inbred lines. Intriguingly, the lines harboring the homozygous C allele exhibit significantly longer EL than that displayed by lines containing the homozygous T allele in three independent populations derived from 647 × ZHENG58, 647 × Mo17 and TY1 × Mo17 (Figs 2f; S11). Indeed, *YIGE1* showed a typical additive effect, with heterozygous lines displaying mid-parent EL. To recapitulate, Chr1.S_50679974 appears to be the causal variation that affects promoter activity, expression of *YIGE1* and finally EL. Chr1.S_50679974 is not located in a known motif or domain, indicating that it may be an unknown regulation site.

The expression of *YIGE1* positively correlates with inflorescence meristem size and ear length

Ear IMs develop into the spikelet pair meristems (SPMs) which then give rise to florets. More florets and higher floret fertility lead to a higher KNPR (Jia *et al.*, 2020). Compared to WT plants, *mum1* mutants displayed significantly reduced IM size ($P = 8.5 \times 10^{-12}$), lower KNPR ($P = 5.2 \times 10^{-7}$) and shorter EL ($P = 7.6 \times 10^{-3}$) before pollination (Fig. 3a–c). By contrast, the OE lines displayed larger IM size ($P = 2.5 \times 10^{-8}$), higher KNPR ($P = 2.8 \times 10^{-4}$) and longer EL ($P = 4.6 \times 10^{-4}$) before pollination than their NT siblings (Fig. 3d–f). Following pollination, c. 59.3% of florets in NT siblings developed into kernels, which is very similar to the proportion observed in OE lines (c. 61.8%; Fig. 3d; Table S2). These findings indicate that the transgenic process did not affect floret fertility, and that more florets in OE lines resulted in more KNPR and longer ears, with KNPR having increased by 16.1% and EL by 10.3% (Table S2).

We next conducted a spatial and temporal expression pattern analysis of *YIGE1* in WT and the *mum1* mutant. The *YIGE1* transcripts were detected in stem, bract, immature and mature leaf, immature root, developing ears (2, 2–5, 5–8 mm), IM, SPM and spikelet meristem (SM). The highest level was observed in the IM. Significant expression differences between the WT and the *mum1* mutant were detected in developing ears, IM, SPM and SM (Fig. 3g), further confirming that differential expression of *YIGE1* in early developing ears and meristems is responsible for EL variation. In addition, *in situ* hybridization showed that *YIGE1* was expressed in IM, SPM and SM (Fig. 3h). Taken together, these results suggest that higher expression of *YIGE1* in the IM results in a larger IM, higher FNPR and longer EL.

YIGE1 is predicted to be involved in sugar and auxin signaling pathways

Considering that *YIGE1* was highly expressed in early developing ears, we conducted RNA-seq using 0.5–1 mm developing ears from OE and NT lines in order to identify the regulatory networks in which *YIGE1* is involved. In total, we detected 506 differentially expressed genes (DEGs, fold change > 2, $P \leq 0.01$), 256 of which were up-regulated, and 250 of which were down-regulated (Fig. 4a). Kyoto Encyclopedia of Genes and Genomes (KEGG) analysis displayed some significantly enriched KEGG pathways ($P < 0.05$), including metabolic pathways, circadian rhythm–plant, starch and sucrose metabolism (Fig. 4b). Moreover, gene ontology (GO) analysis revealed several significantly enriched GO terms (false discovery rate (FDR) < 0.05), including response to hormone, response to abiotic stimulus and post-embryonic development (Fig. 4b). Considering KEGG enrichment on metabolic pathways, and GO enrichment on response to hormone, we therefore subsequently measured the sugar and phytohormones in 2–5 mm developing ears between *YIGE1* NT and OE siblings via GC-MS and LC-MS/MS, respectively. Developing ears from *YIGE1* OE lines accumulated more Indole-3-acetic acid (IAA) than NT plants, and concentrations of several IAA conjugates, including Indole-3-acetyl-L-aspartic acid (IAA-Asp), Indole-3-acetyl glutamic acid (IAA-Glu), and Indole-3-acetyl glycine (IAA-Gly) were similarly increased (Fig. 4c). In addition, gibberellin and 1-Aminocyclopropanecarboxylic acid showed no differences (Table S3). Moreover, significant differences were also observed in concentrations of sucrose, trehalose, D-fructose, glucose and D-sorbitol between *YIGE1* NT and OE siblings, which were decreased in OE developing ears (Fig. 4c). To determine the cause of the reduction in sugar, and an increase in auxin, we investigated the 506 DEGs, finding that several auxin-related genes, including those related to auxin synthesis and transport, and sugar metabolic genes were differentially expressed between the *YIGE1* NT and OE lines (Fig. 4d). Next, we measured the expression levels of these genes using qRT-PCR for NT and OE siblings and found that, consistent with the results in RNA-seq (Fig. S12), these genes showed significant differences in expression levels. Therefore, *YIGE1* may modulate maize inflorescence development via involvement in auxin and sugar signaling (Fig. 4e).

YIGE1 was a target of selection during maize domestication and improvement

Domestication gives rise to a loss of genetic diversity in either the whole genome or in specific regions, meaning that favorable alleles for important traits are enriched (Doebley *et al.*, 2006). Since EL is a key trait of the domestication syndrome, and *YIGE1* plays an important role in affecting natural variations of EL, we postulated that it may be a target of selection during maize domestication. To test this, we used the c. 3 kb region sequence of *YIGE1* in 70 *Zea mays* accessions and 226 landrace accessions. The nucleotide diversity (π) in the 1 kb promoter region of *YIGE1* was much lower in maize than in *Z. mays*, being similar to

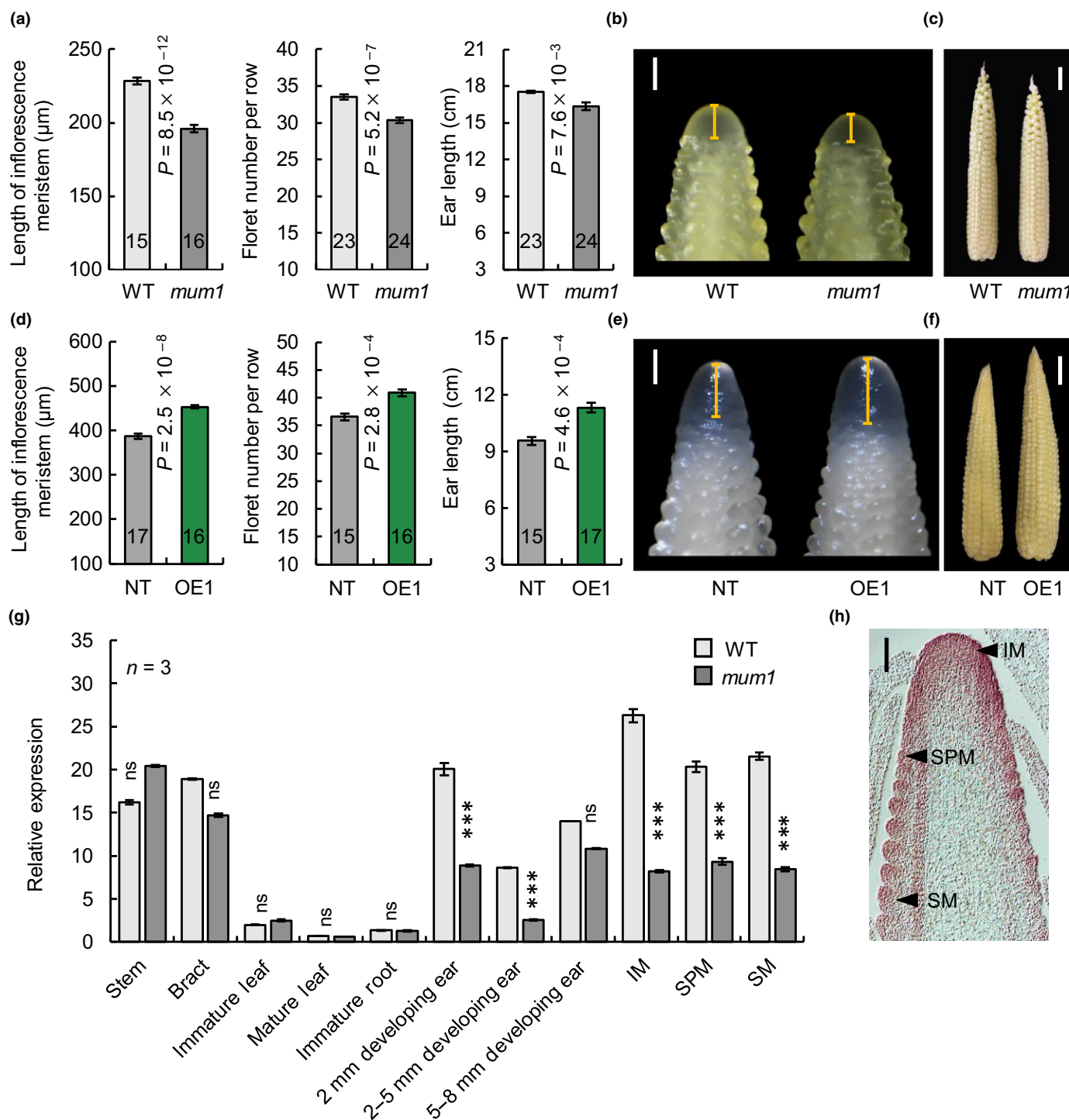


Fig. 3 Function of *YIGE1* in inflorescence size, floret number and ear length (EL). (a, d) The length of the inflorescence meristem (IM), floret number per row and EL, before pollination, in wild-type (WT) and *mum1* mutant lines (a), and overexpression (OE) and nontransgenic (NT) siblings (d), respectively. (b, e) Micrograph of apical 3–4 mm immature ears of WT and *mum1* (b), and OE1 and NT lines (e). Orange lines represent inflorescence meristem length. (c, f) Ear length before pollination in WT and *mum1* (c), and OE1 and NT lines (f). (g) Spatial and temporal expression pattern of *YIGE1* in WT and *mum1* mutant lines. The data in (a, d, g) are mean values \pm SE, and significant differences are determined using one-way analysis of variance (ANOVA). The numbers in each column indicate the sample sizes. (h) mRNA *in situ* hybridization with antisense probes of *YIGE1*. The arrows indicate the IM, spikelet pair meristem (SPM) and spikelet meristem (SM). ***, $P < 0.001$; ns, not significant. Bars: (b, e) 200 μ m; (c, f) 3 cm; (h) 100 μ m.

that found in landraces (Fig. 5a). Tajima's *D* value for the promoter region was negative in maize and *Z. parviglumis* but positive in the landraces. Moreover, Fu and Li's *D* value for this

region deviated significantly from neutrality in maize but did not do so either in *Z. parviglumis* or the landraces. These results suggest that this locus has been subjected to balancing selection in

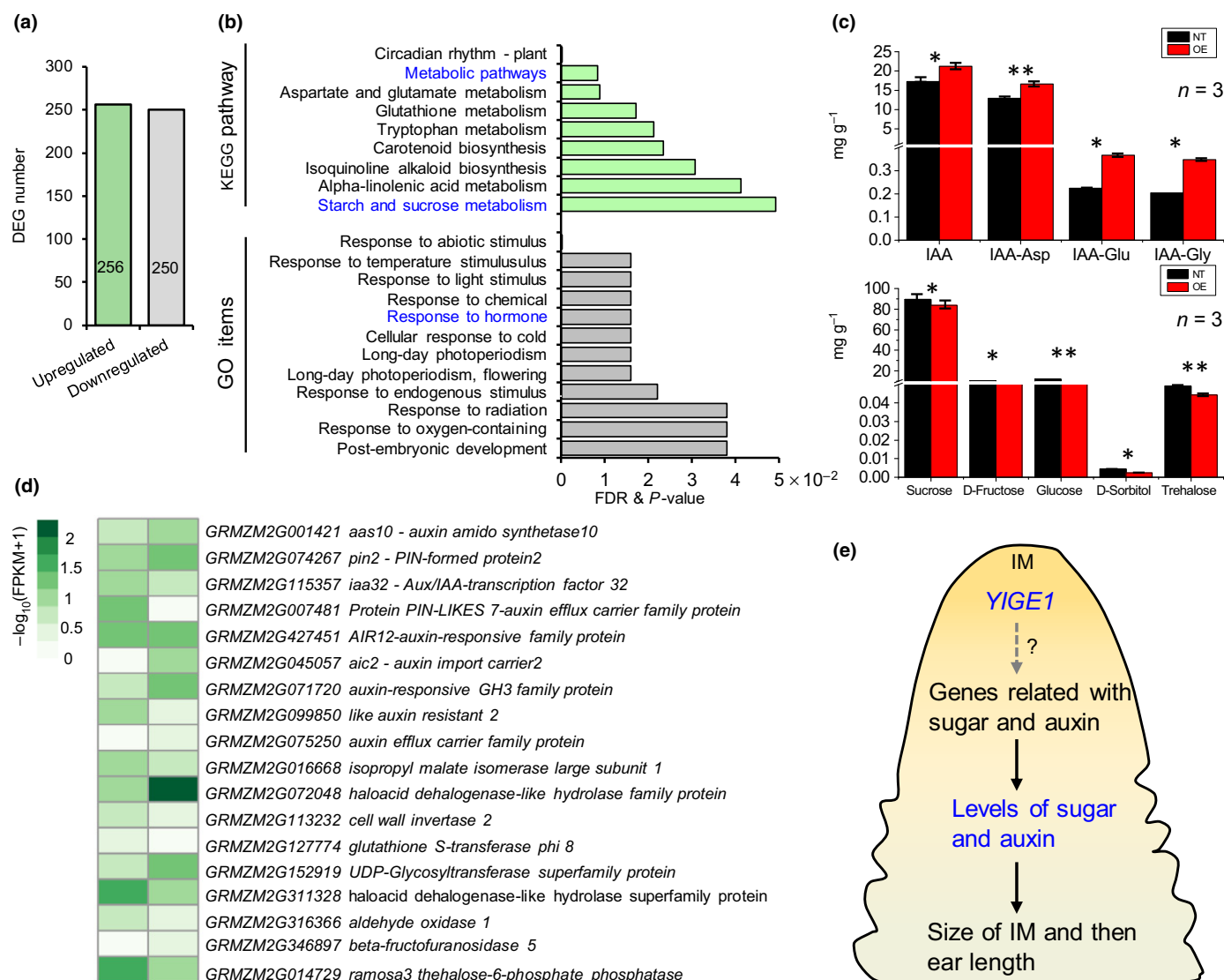


Fig. 4 *YIGE1* may affect ear length (EL) via the regulation of sugar and auxin signaling. (a) The number of differentially expressed genes (DEGs) between nontransgenic (NT) and overexpression (OE) lines was identified using a significant cutoff of $P < 0.01$, and a fold change (FC) > 2 . The numbers of up-regulated and down-regulated DEGs in the OE line are shown. (b) Gene ontology (GO) and Kyoto Encyclopedia of Genes and Genomes (KEGG) analyses revealing the 12 most significantly enriched GO terms in the DEGs, based on false discovery rate (FDR) values, and the nine most significantly enriched KEGG pathways, based on P -values, respectively. (c) The sugar and auxin concentrations in 2–5 mm developing ears from OE and NT siblings. The numbers in each column indicate the sample sizes. The data are mean values \pm SE, and significant differences were determined using one-way analysis of variance (ANOVA). *, $P < 0.05$; **, $P < 0.01$. (d) The differences in transcript levels for the 18 genes related to auxin and sugar signaling in NT and OE siblings, based on $-\log_{10}(\text{FPKM}+1)$, where FPKM is fragments per kilobase of transcript per million mapped reads. (e) Illustration of a proposed model of the regulatory pathways of *YIGE1*.

landraces and directional selection in maize and *Z. parviglumis*. Next, we genotyped 70 *Z. parviglumis* and 226 landrace accessions at Chr1.S_50679974 with Kompetitive Allele-Specific PCR (KASP; Ertiro *et al.*, 2015). The favorable C allele of Chr1.S_50679974 showed a higher frequency in maize inbred lines than in *Z. parviglumis* (0.84 vs 0.56) or landraces (0.84 vs 0.62; Fig. 5b). These results suggest that this locus underwent continuous selection and that the favorable allele was enriched during maize domestication and improvement. However, the intensity of selection is not particularly high, meaning that there is still room for improvement of modern maize.

Ear length exhibits a weakly positive correlation with flowering time (Fig. S13). Long EL may result in late flowering (Danilevskaia *et al.*, 2010). The balance of EL and flowering time is therefore one of the most important considerations in most modern maize breeding programs. We measured another 16 agronomic traits, but only KNPR and grain weight significantly increased without significant effects on flowering time and other agronomic traits in the OE transgenic lines (Fig. 5c; Tables S2, S4). Meanwhile, *YIGE1* showed no correlation with flowering time or any other plant architecture trait in the KO lines, *mum1* mutants or association mapping population (Tables S4, S5).

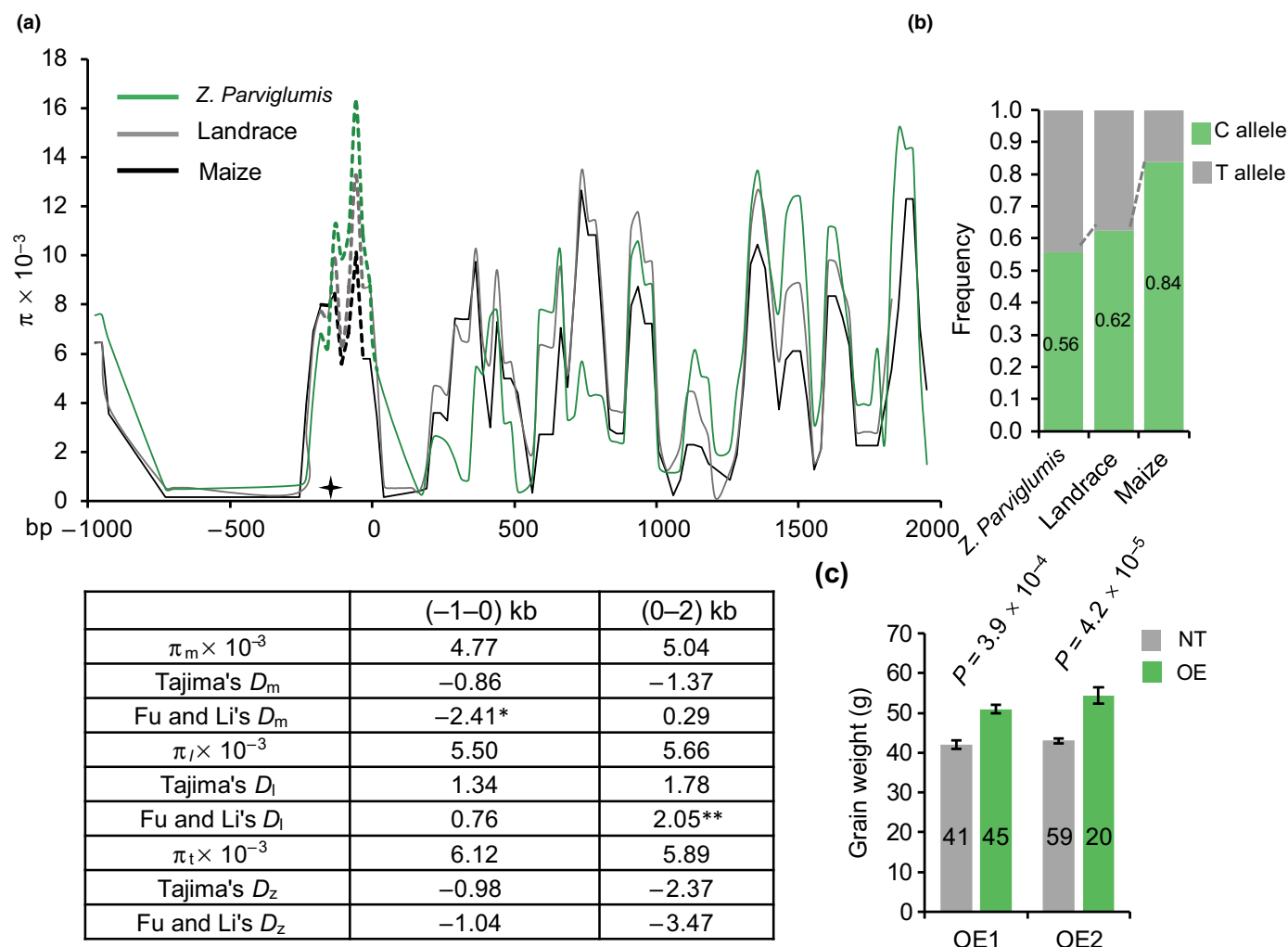


Fig. 5 Nucleotide diversity analysis of *YIGE1* and its potential for increasing yield. (a) Nucleotide diversity (π) at the *YIGE1* locus in *Zea parviglumis*, landrace and maize was calculated using a 100-bp sliding window and 25-bp step size. The black four-pointed star on the x-axis represents the position of Chr1.S_50679974. Tajima's D values and Fu and Li's D values for different regions are shown. *, $P < 0.05$; **, $P < 0.02$. (b) Allele frequency for Chr1.S_50679974 in *Z. parviglumis*, landrace and maize inbred lines. (c) Grain weight for nontransgenic (NT) and *YIGE1* overexpression (OE) siblings in two independent transgenic events. Data are mean values \pm SE, and significant differences were determined using one-way analysis of variance (ANOVA).

These observations indicate that the increased expression of *YIGE1* could enhance EL, KNPR and grain yield without affecting other agronomic traits, suggesting that it has great potential for maize improvement.

Discussion

Ear length, which is a complex agronomic trait, shows a positive correlation with maize grain yield. An increase in EL provides the potential for more kernels per ear, which leads to a higher yield (Huo *et al.*, 2016). However, identification of the genetic components underlying EL is challenging due to the complexity of the maize genome and the difficulty of cloning EL QTLs. A GWAS is a powerful tool for the dissection of complex agronomic traits, and higher marker density and enlarged population size could increase its QTL detection power and resolution (Yan *et al.*, 2011; Yang *et al.*, 2014). In this study, we identified a QTL,

YIGE1, through association mapping (Fig. 1a) which encodes an unknown protein that positively regulates EL by affecting IM activity and pistillate floret number (Figs 1b–i, 4a–f). It thus provides a good example of the power of a GWAS for complex QTL cloning in maize.

YIGE1 has undergone continuous selection; however, the intensity of this selection was relatively mild during maize domestication and improvement, and the favorable allele was significantly enriched in most modern maize inbred lines (Fig. 5a,b). Although the frequency of the favorable haplotype is high, it is not fixed, and about 15% of maize inbred lines could be subjected to more intense selection by molecular breeding in order to improve yield by increasing EL. A KASP molecular marker has been developed (Fig. S11) and could easily be used in breeding. At the same time, *YIGE1* positively regulates EL without negative effects for other agronomic traits (Fig. 1b–i; Table S4). Overexpression of *YIGE1* enhanced EL and grain yield (Fig. 1g–i;

Table S2), suggesting that *YIGE1* affects maize EL via regulation of its expression level and can be better utilized via OE lines in future breeding. CRISPR/Cas9 technology has already shown its superiority in precision breeding through editing the promoter regions of target genes to obtain quantitative variation of important agronomic traits such as fruit size, inflorescence branches, and plant architecture in tomato (Rodriguez-Leal *et al.*, 2017) and yield-related traits in maize (Liu *et al.*, 2021). In present study, the SNP Chr1.S_50679974, located in the promoter of *YIGE1*, had large effects on its promoter strength, expression level and EL (Fig. 3). Therefore, an alternative future approach could be to edit the promoter of *YIGE1* to obtain a super-promoter with a higher expression level that produces longer ears.

Sugar has been shown to act as a signaling molecule that mediates auxin signaling, which regulates the growth of kernels (LeClere *et al.*, 2010), buds (Bertheloot *et al.*, 2020) and roots (Yuan *et al.*, 2020) in plants. However, little is known about the interaction between sugar and auxin signaling in maize inflorescence morphogenesis. *YIGE1* OE lines with larger IMs, higher floret numbers and longer ELs (Fig. 3a–f) showed decreased sugar concentrations and increased auxin concentrations (Fig. 4c), findings that are indicative of the fact that sugar can regulate plant growth (Schluepmann *et al.*, 2004; van Dijken *et al.*, 2004; Satoh-Nagasawa *et al.*, 2006) and low sugar concentrations can promote auxin accumulation (LeClere *et al.*, 2008, 2010). *YIGE1* may be involved in the interactions between sugar and auxin signaling that regulate maize inflorescence development. However, unravelling the exact mechanism by which this is achieved will require considerable future research effort. Auxin plays a critical role in the regulation of floret production in maize ears (Carraro *et al.*, 2006; McSteen *et al.*, 2007; Gallavotti *et al.*, 2008a; Phillips *et al.*, 2011; Jia *et al.*, 2020), consistent with our observation that increasing auxin concentrations generated larger IMs, which are able to accommodate more SPMs, higher numbers of florets per row, and ultimately a higher KNPR, longer EL and higher grain yield (Figs 3–5). The plant growth hormone auxin controls cell identity, division, and expansion (Yuan *et al.*, 2020). However, it is not known whether the larger IM is a result of cell division or expansion, because it is difficult to directly measure the cell number and cell size in the IM. *YIGE1* is a cytoplasmic protein (Fig. S6c), which renders it very unlikely that *YIGE1* regulates other genes at the transcriptional stage. Hence, we speculate that the *YIGE1* protein may function in complexes to regulate maize inflorescence and ear development. We used a yeast two hybrid assay with *YIGE1* as a relatively quick method of detecting protein–protein interactions. A total of seven potential interactions were detected (Table S6), and four were further selected (based on expression patterns and predicted subcellular localization) for verification by yeast two hybrid and luciferase complementation assay in tobacco (Table S6). Unfortunately, none of them was verified by further point to point screening. In addition, *YIGI1* has no known domains, which renders effective antibody synthesis difficult, meaning that it is not easy for us to directly detect the proteins which interact with *YIGE1*. Analyzing how *YIGE1* alters the concentrations of sugar and auxin to

regulate maize inflorescence development not only deepens our understanding of its molecular mechanism, but also provides a novel route for the genetic improvement of maize.









Acknowledgements

This research was supported by the National Natural Science Foundation of China (31961133002) and the National Key Research and Development Program of China (2020YFE0202300).

Author contributions

JBY designed and supervised this study. YLuo, MLZ, YLiu and WQL performed the field trials. YLuo, YP, MJ and WJW performed the data analysis, including association mapping, RNA-seq and selection analysis. YLuo, MLZ, LMJ and JY carried out validation of gene function and gene expression analysis. YLuo, JL, GSC, ARF and JBY wrote and revised the manuscript. YLuo and all the authors read and approved the paper. YLuo and MLZ contributed equally.

ORCID

Alisdair R. Fernie  <https://orcid.org/0000-0001-9000-335X>
Liumei Jian  <https://orcid.org/0000-0001-6234-9265>
Jie Liu  <https://orcid.org/0000-0002-1129-9584>
Yun Luo  <https://orcid.org/0000-0003-2732-5916>
Yong Peng  <https://orcid.org/0000-0002-5379-4348>
Wenjie Wei  <https://orcid.org/0000-0003-4105-9693>
Jianbing Yan  <https://orcid.org/0000-0001-8650-7811>
Mingliang Zhang  <https://orcid.org/0000-0003-0618-4640>

Data availability

The full genomic sequence of *GRMZM2G008490* can be found in GenBank (accession no. OK321185). The transcriptome data have been deposited in National Center for Biotechnology Information's (NCBI) Sequence Read Archive with accession no. PRJNA776742.

References

- Barrett JC, Fry B, Maller J, Daly MJ. 2005. Haploview: analysis and visualization of LD and haplotype maps. *Bioinformatics* 21: 263–265.
- Bertheloot J, Barbier F, Boudon F, Perez-Garcia MD, Peron T, Citerne S, Dun E, Beveridge C, Godin C, Sakr S. 2020. Sugar availability suppresses the auxin-induced strigolactone pathway to promote bud outgrowth. *New Phytologist* 225: 866–879.
- Bolger AM, Lohse M, Usadel B. 2014. Trimmomatic: a flexible trimmer for Illumina sequence data. *Bioinformatics* 30: 2114–2120.
- Bradbury PJ, Zhang Z, Kroon DE, Casstevens TM, Ramdoss Y, Buckler ES. 2007. TASSEL: software for association mapping of complex traits in diverse samples. *Bioinformatics* 23: 2633–2635.
- Carraro N, Forestan C, Canova S, Traas J, Varotto S. 2006. *ZmPIN1a* and *ZmPIN1b* encode two novel putative candidates for polar auxin transport and plant architecture determination of maize. *Plant Physiology* 142: 254–264.

- Claeys H, Vi SL, Xu X, Satoh-Nagasawa N, Eveland AL, Goldshmidt A, Feil R, Beggs GA, Sakai H, Brennan RG *et al.* 2019. Control of meristem determinacy by trehalose 6-phosphate phosphatases is uncoupled from enzymatic activity. *Nature Plants* 5: 352–357.
- Danilevskaya ON, Meng X, Ananiev EV. 2010. Concerted modification of flowering time and inflorescence architecture by ectopic expression of *TFL1*-like genes in maize. *Plant Physiology* 153: 238–251.
- Dauphin CE, Durand A, Lubonis K, Wortham H, Dron J. 2020. Quantification of monosaccharide anhydrides by gas chromatography/mass spectrometry in lichen samples. *Journal of Chromatography A* 1612: 460675.
- van Dijken AJ, Schlupmann H, Smeeke SC. 2004. *Arabidopsis trehalose-6-phosphate synthase 1* is essential for normal vegetative growth and transition to flowering. *Plant Physiology* 135: 969–977.
- Doebley JF, Gaut BS, Smith BD. 2006. The molecular genetics of crop domestication. *Cell* 127: 1309–1321.
- Ertiro BT, Ogugo V, Worku M, Das B, Olsen M, Labuschagne M, Semagn K. 2015. Comparison of kompetitive allele specific PCR (KASP) and genotyping by sequencing (GBS) for quality control analysis in maize. *BMC Genomics* 16: 908.
- Flint-Garcia SA, Thornsberry JM, Buckler ES. 2003. Structure of linkage disequilibrium in plants. *Annual Review of Plant Biology* 54: 357–374.
- Flint-Garcia SA, Thuillet AC, Yu J, Pressoir G, Romero SM, Mitchell SE, Doebley J, Kresovich S, Goodman MM, Buckler ES. 2005. Maize association population: a high-resolution platform for quantitative trait locus dissection. *The Plant Journal* 44: 1054–1064.
- Floková K, Tarkowská D, Miersch O, Strnad M, Wasternack C, Novák O. 2014. UHPLC-MS/MS based target profiling of stress-induced phytohormones. *Phytochemistry* 105: 147–157.
- Gallavotti A, Barazesh S, Malcomber S, Hall D, Jackson D, Schmidt RJ, McSteen P. 2008a. *Sparse inflorescence1* encodes a monocot-specific YUCCA-like gene required for vegetative and reproductive development in maize. *Proceedings of the National Academy of Sciences, USA* 105: 15196–15201.
- Gallavotti A, Yang Y, Schmidt RJ, Jackson D. 2008b. The relationship between auxin transport and maize branching. *Plant Physiology* 147: 1913–1923.
- Galli M, Liu Q, Moss BL, Malcomber S, Li W, Gaines C, Federici S, Roshkovan J, Meeley R, Nemhauser JL *et al.* 2015. Auxin signaling modules regulate maize inflorescence architecture. *Proceedings of the National Academy of Sciences, USA* 112: 13372–13377.
- Gerland P, Raftery AE, Ševčíková H, Li N, Gu D, Spoorenberg T, Alkema L, Fosdick BK, Chunn J, Lalic N *et al.* 2014. World population stabilization unlikely this century. *Science* 346: 234–237.
- Ghosh S, Chan CK. 2016. Analysis of RNA-seq data using tophat and cufflinks. *Methods in Molecular Biology* 1374: 339–361.
- Gómez-González S, Ruiz-Jiménez J, Priego-Capote F, Luque de Castro MD. 2010. Qualitative and quantitative sugar profiling in olive fruits, leaves, and stems by gas chromatography-tandem mass spectrometry (GC-MS/MS) after ultrasound-assisted leaching. *Journal Agricultural and Food Chemistry* 58: 12292–12299.
- Hawkins E, Fricker TE, Challinor AJ, Ferro CA, Ho CK, Osborne TM. 2013. Increasing influence of heat stress on French maize yields from the 1960s to the 2030s. *Global Change Biology* 19: 937–947.
- Huang C, Sun H, Xu D, Chen Q, Liang Y, Wang X, Xu G, Tian J, Wang C, Li D *et al.* 2018. *ZmCCT9* enhances maize adaptation to higher latitudes. *Proceedings of the National Academy of Sciences, USA* 115: E334–E341.
- Hung HY, Shannon LM, Tian F, Bradbury PJ, Chen C, Flint-Garcia SA, McMullen MD, Ware D, Buckler ES, Doebley JF *et al.* 2012. *ZmCCT* and the genetic basis of day-length adaptation underlying the postdomestication spread of maize. *Proceedings of the National Academy of Sciences, USA* 109: E1913–E1921.
- Huo D, Ning Q, Shen X, Liu L, Zhang Z. 2016. QTL Mapping of kernel number-related traits and validation of one major QTL for ear length in maize. *PLoS ONE* 11: e0155506.
- Jackson D, Hake S. 1999. Control of phyllotaxy in maize by the *abphyll1* gene. *Development* 126: 315–323.
- Jia H, Li M, Li W, Liu L, Jian Y, Yang Z, Shen X, Ning Q, Du Y, Zhao R *et al.* 2020. A serine/threonine protein kinase encoding gene *KERNEL NUMBER PER ROW6* regulates maize grain yield. *Nature Communications* 11: 988.
- Kim D, Pertea G, Trapnell C, Pimentel H, Kelley R, Salzberg SL. 2013. TopHat2: accurate alignment of transcriptomes in the presence of insertions, deletions and gene fusions. *Genome Biology* 14: R36.
- LeClere S, Schmelz EA, Chourey PS. 2008. Cell wall invertase-deficient miniature1 kernels have altered phytohormone levels. *Phytochemistry* 69: 692–699.
- LeClere S, Schmelz EA, Chourey PS. 2010. Sugar levels regulate tryptophan-dependent auxin biosynthesis in developing maize kernels. *Plant Physiology* 153: 306–318.
- Li C, Liu C, Qi X, Wu Y, Fei X, Mao L, Cheng B, Li X, Xie C. 2017. RNA-guided Cas9 as an *in vivo* desired-target mutator in maize. *Plant Biotechnology Journal* 15: 1566–1576.
- Li H, Peng Z, Yang X, Wang W, Fu J, Wang J, Han Y, Chai Y, Guo T, Yang N *et al.* 2013. Genome-wide association study dissects the genetic architecture of oil biosynthesis in maize kernels. *Nature Genetics* 45: 43–50.
- Li M, Zhong W, Yang F, Zhang Z. 2018. Genetic and molecular mechanisms of quantitative trait loci controlling maize inflorescence architecture. *Plant and Cell Physiology* 59: 448–457.
- Li W, Yu Y, Wang L, Luo Y, Peng Y, Xu Y, Liu X, Wu S, Jian L, Xu J *et al.* 2021. The genetic architecture of the dynamic changes in grain moisture in maize. *Plant Biotechnology Journal* 19: 1195–1205.
- Li Y, Zhou C, Yan X, Zhang J, Xu J. 2016. Simultaneous analysis of ten phytohormones in *Sargassum horneri* by high-performance liquid chromatography with electrospray ionization tandem mass spectrometry. *Journal of Separation Science* 39: 1804–1813.
- Liang Y, Liu HJ, Yan J, Tian F. 2021. Natural variation in crops: realized understanding, continuing promise. *Annual Review of Plant Biology* 72: 357–385.
- Lincoln C, Long J, Yamaguchi J, Serikawa K, Hake S. 1994. A *knotted1*-like homeobox gene in *Arabidopsis* is expressed in the vegetative meristem and dramatically alters leaf morphology when overexpressed in transgenic plants. *Plant Cell* 6: 1859–1876.
- Liu H, Ding Y, Zhou Y, Jin W, Xie K, Chen LL. 2017a. CRISPR-P 2.0: an improved CRISPR-Cas9 tool for genome editing in plants. *Molecular Plant* 10: 530–532.
- Liu H-J, Jian L, Xu J, Zhang Q, Zhang M, Jin M, Peng Y, Yan J, Han B, Liu J *et al.* 2020. High-throughput CRISPR/Cas9 mutagenesis streamlines trait gene identification in maize. *Plant Cell* 32: 1397–1413.
- Liu H, Luo X, Niu L, Xiao Y, Chen LU, Liu J, Wang X, Jin M, Li W, Zhang Q *et al.* 2017b. Distant eQTLs and non-coding sequences play critical roles in regulating gene expression and quantitative trait variation in maize. *Molecular Plant* 10: 414–426.
- Liu J, Huang J, Guo H, Lan L, Wang H, Xu Y, Yang X, Li W, Tong H, Xiao Y *et al.* 2017. The conserved and unique genetic architecture of kernel size and weight in maize and rice. *Plant Physiology* 175: 774–785.
- Liu L, Gallagher J, Arevalo ED, Chen R, Skopelitis T, Wu Q, Bartlett M, Jackson D. 2021. Enhancing grain-yield-related traits by CRISPR-Cas9 promoter editing of maize *CLE* genes. *Nature Plants* 7: 287–294.
- Mao H, Wang H, Liu S, Li Z, Yang X, Yan J, Li J, Tran LS, Qin F. 2015. A transposable element in a *NAC* gene is associated with drought tolerance in maize seedlings. *Nature Communications* 6: 8326.
- McSteen P, Hake S. 2001. *Barren inflorescence2* regulates axillary meristem development in the maize inflorescence. *Development* 128: 2881–2891.
- McSteen P, Malcomber S, Skirpan A, Lunde C, Wu X, Kellogg E, Hake S. 2007. *Barren inflorescence2* encodes a co-ortholog of the PINOID serine/threonine kinase and is required for organogenesis during inflorescence and vegetative development in maize. *Plant Physiology* 144: 1000–1011.
- Ning Q, Jian Y, Du Y, Li Y, Shen X, Jia H, Zhao R, Zhan J, Yang F, Jackson D *et al.* 2021. An ethylene biosynthesis enzyme controls quantitative variation in maize ear length and kernel yield. *Nature Communications* 12: 5832.
- Phillips KA, Skirpan AL, Liu X, Christensen A, Slewinski TL, Hudson C, Barazesh S, Cohen JD, Malcomber S, McSteen P. 2011. *Vanishing tassel2* encodes a grass-specific tryptophan aminotransferase required for vegetative and reproductive development in maize. *Plant Cell* 23: 550–566.
- Price AH. 2006. Believe it or not, QTLs are accurate! *Trends in Plant Science* 11: 213–216.

- Rao X, Huang X, Zhou Z, Lin X. 2013. An improvement of the $2^{-\Delta\Delta CT}$ method for quantitative real-time polymerase chain reaction data analysis. *Biostatistics, Bioinformatics and Biomathematics* 3: 71–85.
- Ray DK, Mueller ND, West PC, Foley JA. 2013. Yield trends are insufficient to double global crop production by 2050. *PLoS ONE* 8: e66428.
- Rodriguez-Leal D, Lemmon ZH, Man J, Bartlett ME, Lippman ZB. 2017. Engineering quantitative trait variation for crop improvement by genome editing. *Cell* 171: 470–480.
- Sato N, Nagasawa N, Nagasawa N, Malcomber S, Sakai H, Jackson D. 2006. A trehalose metabolic enzyme controls inflorescence architecture in maize. *Nature* 441: 227–230.
- Shindelin J, Rueden CT, Hiner MC, Eliceiri KW. 2015. The ImageJ ecosystem: an open platform for biomedical image analysis. *Molecular Reproduction Development* 82: 518–529.
- Schluppmann H, van Dijken A, Aghdasi M, Wobbes B, Paul M, Smeekens S. 2004. Trehalose mediated growth inhibition of *Arabidopsis* seedlings is due to trehalose-6-phosphate accumulation. *Plant Physiology* 135: 879–890.
- Šimura J, Antoniadis I, Široká J, Tarkowská D, Strnad M, Ljung K, Novák O. 2018. Plant hormonomics: multiple phytohormone profiling by targeted metabolomics. *Plant Physiology* 177: 476–489.
- Skirpan A, Culler AH, Gallavotti A, Jackson D, Cohen JD, McSteen P. 2009. BARREN INFLORESCENCE2 interaction with ZmPIN1a suggests a role in auxin transport during maize inflorescence development. *Plant and Cell Physiology* 50: 652–657.
- Tian T, Liu Y, Yan H, You Q, Yi X, Du Z, Xu W, Su Z. 2017. AGRIGO v2.0: a GO analysis toolkit for the agricultural community, 2017 update. *Nucleic Acids Research* 45: W122–W129.
- Varet H, Brillet-Guéguen L, Coppée JY, Dillies MA. 2016. SARTools: a DESeq2- and edgeR-based R pipeline for comprehensive differential analysis of RNA-Seq data. *PLoS ONE* 11: e0157022.
- Wang X, Wang H, Liu S, Ferjani A, Li J, Yan J, Yang X, Qin F. 2016. Genetic variation in *ZmVPP1* contributes to drought tolerance in maize seedlings. *Nature Genetics* 48: 1233–1241.
- Xiao Y, Liu H, Wu L, Warburton M, Yan J. 2017. Genome-wide association studies in maize: praise and stargaze. *Molecular Plant* 10: 359–374.
- Xiao Y, Tong H, Yang X, Xu S, Pan Q, Qiao F, Raihan MS, Luo Y, Liu H, Zhang X *et al.* 2016. Genome-wide dissection of the maize ear genetic architecture using multiple populations. *New Phytologist* 210: 1095–1106.
- Yan J, Kandianis CB, Harjes CE, Bai L, Kim EH, Yang X, Skinner DJ, Fu Z, Mitchell S, Li Q *et al.* 2010. Rare genetic variation at *Zea mays crtRB1* increases beta-carotene in maize grain. *Nature Genetics* 42: 322–327.
- Yan J, Warburton M, Crouch J. 2011. Association mapping for enhancing maize (*Zea mays* L.) genetic improvement. *Crop Science* 51: 433–449.
- Yang N, Lu Y, Yang X, Huang J, Zhou Y, Ali F, Wen W, Liu J, Li J, Yan J. 2014. Genome wide association studies using a new nonparametric model reveal the genetic architecture of 17 agronomic traits in an enlarged maize association panel. *PLoS Genetics* 10: e1004573.
- Yang Q, Li Z, Li W, Ku L, Wang C, Ye J, Li K, Yang N, Li Y, Zhong T *et al.* 2013. CACTA-like transposable element in *ZmCCT* attenuated photoperiod sensitivity and accelerated the postdomestication spread of maize. *Proceedings of the National Academy of Sciences, USA* 110: 16969–16974.
- Yang X, Gao S, Xu S, Zhang Z, Prasanna BM, Li L, Li J, Yan J. 2011. Characterization of a global germplasm collection and its potential utilization for analysis of complex quantitative traits in maize. *Molecular Breeding* 28: 511–526.
- Yoo SD, Cho YH, Sheen J. 2007. *Arabidopsis* mesophyll protoplasts: a versatile cell system for transient gene expression analysis. *Nature Protocols* 2: 1565–1572.
- Yu H, Li J. 2021. Short- and long-term challenges in crop breeding. *Nature Science Review* 8: nwab002.
- Yu J, Pressoir G, Briggs WH, Vroh Bi I, Yamasaki M, Doebley JF, McMullen MD, Gaut BS, Nielsen DM, Holland JB *et al.* 2006. A unified mixed-model method for association mapping that accounts for multiple levels of relatedness. *Nature Genetics* 38: 203–208.
- Yuan X, Xu P, Yu Y, Xiong Y. 2020. Glucose-TOR signaling regulates PIN2 stability to orchestrate auxin gradient and cell expansion in *Arabidopsis* root. *Proceedings of the National Academy of Sciences, USA* 117: 32223–32225.
- Zhang D, Yuan Z. 2014. Molecular control of grass inflorescence development. *Annual Review of Plant Biology* 65: 553–578.
- Zhang D, Zhou G, Liu B, Kong Y, Chen N, Qiu Q, Yin H, An J, Zhang F, Chen F. 2011. *HCF243* encodes a chloroplast-localized protein involved in the D1 protein stability of the Arabidopsis photosystem II complex. *Plant Physiology* 157: 608–619.
- Zhang Z, Ersoz E, Lai C-Q, Todhunter RJ, Tiwari HK, Gore MA, Bradbury PJ, Yu J, Arnett DK, Ordovas JM *et al.* 2010. Mixed linear model approach adapted for genome-wide association studies. *Nature Genetics* 42: 355–360.
- Zhao Y. 2010. Auxin biosynthesis and its role in plant development. *Annual Review of Plant Biology* 61: 49–64.
- Zhu XM, Shao XY, Pei YH, Guo XM, Li J, Song XY, Zhao MA. 2018. Genetic diversity and genome-wide association study of major ear quantitative traits using high-density SNPs in maize. *Frontiers in Plant Science* 9: 966.

Supporting Information

Additional Supporting Information may be found online in the Supporting Information section at the end of the article.

Fig. S1 Ear length (EL) variations in maize inbred lines from the association mapping panel.

Fig. S2 The 432 bp deletion and phenotype of ear length (EL) in *GRMZM2G008490* knockout (KO) lines.

Fig. S3 Editing type by Cas9 and phenotype of ear length (EL) in *GRMZM2G329040*, *GRMZM2G703565* and *AC208571.4_FG001* KO lines.

Fig. S4 Phenotype of ear length (EL) in the *GRMZM2G008490* *mum1* mutant.

Fig. S5 Phenotype of ear length (EL) in *GRMZM2G008490* overexpression (OE) lines.

Fig. S6 Phylogenetic analysis and subcellular localization of YIG1.

Fig. S7 Plant architecture of the *mum1*, overexpression (OE) and knockout (KO) lines of YIG1.

Fig. S8 Genetic polymorphisms of YIG1.

Fig. S9 Conditional association analysis using Chr1.S_50679974 as a covariant.

Fig. S10 Expression level of YIG1 and ear length (EL) variations in maize inbred lines.

Fig. S11 Identification of the genotype of Chr1.S_50679974 in three F₂ : 3 segregation populations.

Fig. S12 Measurement of differentially expressed gene (DEG) expression levels by quantitative real-time polymerase chain reaction (qRT-PCR).

Fig. S13 The correlation between ear length and flowering traits.

Table S1 Primers used in this experiment.

Table S2 Phenotypes of ear-related traits of transgenic lines.

Table S3 Sugar and phytohormone content in 2–5 mm developing ears for *YIGE1* nontransgenic (NT) and overexpression (OE) siblings.

Table S4 Phenotype of agronomic traits of transgenic lines and *mum1* lines.

Table S5 Phenotype of flowing-related traits and plant architecture-related traits in the association population based on the lead single-nucleotide polymorphism (SNP), Chr1.S_50679974.

Table S6 Potential YIGE1 interaction proteins.

Please note: Wiley Blackwell are not responsible for the content or functionality of any Supporting Information supplied by the authors. Any queries (other than missing material) should be directed to the *New Phytologist* Central Office.



About New Phytologist

- *New Phytologist* is an electronic (online-only) journal owned by the New Phytologist Foundation, a **not-for-profit organization** dedicated to the promotion of plant science, facilitating projects from symposia to free access for our Tansley reviews and Tansley insights.
- Regular papers, Letters, Viewpoints, Research reviews, Rapid reports and both Modelling/Theory and Methods papers are encouraged. We are committed to rapid processing, from online submission through to publication 'as ready' via *Early View* – our average time to decision is <23 days. There are **no page or colour charges** and a PDF version will be provided for each article.
- The journal is available online at Wiley Online Library. Visit **www.newphytologist.com** to search the articles and register for table of contents email alerts.
- If you have any questions, do get in touch with Central Office (np-centraloffice@lancaster.ac.uk) or, if it is more convenient, our USA Office (np-usaoffice@lancaster.ac.uk)
- For submission instructions, subscription and all the latest information visit **www.newphytologist.com**

See also the Commentary on this article by Cowling & Kelley, **234**: 337–339.